ASTRONOMY & ASTROPHYSICS
SUPPLEMENT SERIES

Astron. Astrophys. Suppl. Ser. **93,** 449-462 (1992)

Narrow band multicolor photometry of reddened and unreddened early-type stars.*

P.A. Bastiaansen

Sterrewacht Leiden, Huygens Laboratory, Postbus 9513, 2300 RA Leiden, the Netherlands

Received February 6; accepted August 23, 1991

Abstract. — Photometric observations of reddened and unreddened southern hemisphere stars are reported in this paper. The wavelength range was 340-787 nm, covered by 20 discrete filter passbands of 4 to 11 nm width. Results are presented as magnitudes relative to the Hayes-Latham calibration of Vega. Interstellar extinction curves are derived for 19 stars. It is demonstrated that a number of shallow features exist in the extinction curves, relative to a straight line approximation. The investigation forms part of a larger program including polarization observations.

Key words: interstellar medium: extinction — photometry.

1. Introduction.

The existence of a very broadband structure in the interstellar extinction curve in the visible region seems well established. Independent observational evidence has been reported by several authors (Whiteoak 1966; Rex 1974; Van Breda *et al.* 1981). A common feature found by all observers is a dip in the extinction curve around 560 nm $(\lambda^{-1} = 1.8\ \mu^{-1})$ with a width of 100 to 200 nm. The strength of the feature has been shown to be correlated with total reddening (Hayes *et al.* 1973). Theoretical interpretation of the phenomenon has concentrated on calculating the effects of impurities embedded in interstellar dust grains. Such calculations predict similar broad band structure in the interstellar polarization curves (Hayes *et al.* 1973).

Another and better-known feature is the change in slope of the extinction curve around $\lambda = 440$ nm $(\lambda^{-1} = 2.3\ \mu^{-1})$ which can be explained in terms of a size distribution of the grains. This size distribution in turn will also show up in interstellar polarization curves (e.g. λ_{max}).

It is thus clear that any serious attempt to construct a theoretical model for interstellar dust should take into account both extinction and polarization phenomena. A range of models is available to describe different sets of basic observations. Definite conclusions, however, cannot be made, due to the fact that there is only a small number of stars for which a complete set of stokes parameters has been observed over a reasonable wavelength range. An observational program was therefore initiated at the Leiden Observatory to measure interstellar extinction as well as linear and, if possible, circular polarization for a number of stars. The present article will describe the photometric measurements and derive the interstellar extinction curves. A further discussion of the extinction features will be published in a later article, in relation to features in the polarization curves.

2. The observations.

Narrow band photometric observations of 19 reddened stars and of a number of stars with small reddening were made during 14 nights in february 1979 with a single channel photometer, attached to the ESO 50 cm. telescope of La Silla Observatory. Tables 1(a) and 1(b) provide a list of the observed stars, together with MK and *UBV* data gathered from the literature. Main sources were Nicolet (1978) for *UBV* data, Jaschek *et al.* (1964) and Kennedy *et al.* (1974) for MK spectral types. The passbands were defined by 20 interference filters, for which relevant data are given in Table 2, Columns 1 through 4. The bands were chosen so as to avoid all hydrogen lines (except for the filter at 378 nm) and some strong lines of HeI, HeII; the absorption bands of atmospheric oxygen (690 and 764 nm) are also avoided. Figure 1 shows the form of the passbands and the position of the main line features. For measurements with the filters 340 nm through 520 nm an EMI 6256B photomultiplier (with S-11 cathode and

* Based on observations obtained at the European Southern Observatory, La Silla, Chile.

quartz entrance window) was used. This multiplier was thermo-electrically cooled down to $-20°$ C. The red part of the spectrum (541 through 787 nm) was measured with an EMI 9558B (S-20 cathode), cooled to dry ice temperature. Because of the low quantum efficiency (only 2% at 800 nm) the photometric accuracy at the longer wavelengths was reduced for the fainter stars.

A measurement on a star (or sky) was always made with a short sequence of filters. The integration time per filter would typically be 15-20 seconds and the filter at 450 nm was always included as a reference for measurements with both multipliers. The standard diaphragm used was 30" in diameter. Occasionally a smaller size had to be used (15" or 21"). The required (small) magnitude correction has been determined from suitable pairs of observations. Part of the observations on very bright stars could be made only with an optical attenuator in the beam in order not to exceed the maximum allowed anode current and also to reduce the counter dead time correction. After some experimentation (also with a neutral density filter), it was decided to use a simple circular flange attached to the top of the telescope tube, which obscured the outer parts of the primary mirror. This changes the diffraction pattern in the focal plane of the telescope and the image of the pupil on the photomultiplier and consequently one is essentially working in a different photometric system. Additional observations were made to determine the wavelength dependent zeropoint shift between the two systems.

For the determination of atmospheric extinction, a set of 9 stars was chosen from the system of Walraven standard stars. These stars are HD 17081, 36512, 41534, 49798, 74575, 87504, 104337, 122980 and 144470. Analysis of measurements in the Walraven system, extending over many years, has shown that any variations in these standard stars are certainly small enough to be neglected over a period of a few weeks (Lub & Pel 1977); it is assumed that this also holds in the longer wavelength region which is not covered by the Walraven bands. In general, the frequency of extinction observations was at least once per hour.

3. Reduction.

Determination of atmospheric extinction and instrumental zeropoint was done in two steps.

(a) Relative magnitudes of the 9 extinction standards in the 20 color system were determined in an iterative way simultaneously with the determination of nightly extinction coefficients and the nightly zeropoint for the magnitude scale in each filter. The determination of relative magnitudes for the standards was made less dependent on atmospheric extinction and instrumental stability by using only selected pairs of observations. Criteria were: both observations made within a short time (less than 15 minutes apart) and at about the same small zenith distance (sec $z < 1.5$; Δ sec $z < 0.1$). Small time-dependent but systematic corrections were found to be needed on some nights for the extinction coefficient and the zeropoint. This reduction step was limited to observations made without the flange on the telescope.

(b) Observations made with the flange on the telescope were transformed to equivalent magnitudes in the system without a flange. The required transformation terms were determined from suitable pairs of observations typically made within a time span of 10 minutes and at a small zenith distance. The transformed observations were then reduced separately, using relative magnitudes for the standard stars as determined in step (a) above. Resulting extinction and zeropoints were checked for consistency with the results of steps (a).

All individual measurements could thus be reduced to relative magnitudes outside the atmosphere. Then, for each sequence of measurements, magnitude differences relative to the standard reference filter at 450 nm were calculated. This should effectively remove any residual slow color independent variations of, for instance, photometer response, extinction, or stellar brightness. Finally, all magnitude differences were averaged per star and per filter.

The resulting list of relative magnitudes may be used directly to derive interstellar extinction curves. However, in order to make the observations more generally useful, these have been converted to the Hayes-Latham calibration of Vega. As a main reference source, the compilation by Breger (1976) has been used. For the wavelength range 340-582 nm, three stars from Breger's list of secondary standards were used to find the conversion terms: HD 74280 (η Hya), HD 87901 (α Leo) and HD 100889 (Θ Crt). No calibration of these secondary standards is given for the range 611-787 nm; the Oke measurements of HD 37128 (ϵ Ori) and HD 87901 (α Leo), as calibrated by Breger were used. From this set of absolute standards the mean conversion term (zeropoint shift) was calculated for each filter. An exception is $\lambda = 378$ nm. No absolute calibration exists for this wavelength. An estimate was obtained instead by interpolating the energy distribution of an early O star (HD 66811 was used for this purpose). Resulting magnitudes on the Hayes-Latham system of absolute calibration are listed in Table 3, relative to a zeropoint at 500 nm. The table gives for each star/filter combination: the magnitude m_ν, the mean (internal) error, and N which is the number of "independent observations" used to calculate the mean error. N is equal to the actual number of observations for the extinction sample stars while for the standard stars, N is the number of nights on which the star was used for determination of the atmospheric extinction coefficient. Results based on observations of only one night, are indicated with an asterisk in Table 3.

Table 4 shows the rms deviations of the present data relative to the Breger/Oke data based on the set of stars as used above to determine the required zeropoint shift. In addition a comparison has been made between the present data and the system of standards as observed and calibrated by Tüg (1978, 1980). Stars in common are HD 37128, HD 66811, HD 74280 and HD 87901. Results (Tab. 4) show that, apart from a constant zeropoint shift, systematic wavelength dependent differences of up to 0.04 magnitudes exist. This is not extreme, considering the passband differences both in position and in width and the resulting differential influence of stellar lines. A comparison of the system of Hayes-Latham with that of Tüg, both based on independent calibration of Vega, also shows wavelength dependent differences of up to 0.03 magnitudes. The rms deviations shown in Table 4 indicate an internal consistency of the present observations of at least 0.015 magnitudes, the larger deviations coinciding with the position of the Balmer jump and helium lines where passband differences play a role.

Extensive laboratory measurements of the peak and sideband filter transmissions have been made. These were combined with the response curves of the photomultipliers and with the measured energy distribution of the program stars. As a result, an upper limit is established for the effect of sideband transmission integrated over the full wavelength range of photometer sensitivity for each star. There was a marginally significant blue leak for only one (infrared) filter. All possibly relevant sideband effects are listed in Table 2, together with strong stellar lines in or near the passbands; strong discontinuities in energy distribution are also mentioned. From these effects a worst-case calculation provides an estimate of the maximum deviations due to sideband filter transmission, of the energy distributions relative to the true stellar continua for the spectral type range O to early A. These maximum deviations are entered in Table 2, Column 5 (Δm). Effects, calculated to be smaller than 0.01 magnitude, are rounded upwards to 0.01 in the table. Note that the data have not been corrected for these effects; they are given only in order to be able to judge the differences between the present observations and other published data, such as narrow-band scanner observations.

The wavelength calibration is also important, as a wrong determination of effective wavelength for one single filter way eventually show up as an "interstellar extinction feature" present in all extinction curves. Effective wavelengths, as listed in Table 2 (Col. 1), were determined from the passband profiles with an accuracy of better than 0.3 nm. An error of 0.3 nm would, in the normalized extinction curve (see further on), correspond to an extinction feature of 0.003 magnitude at 400 nm or 0.001 magnitude at 700 nm. Possible shifts in effective wavelength caused by filter tilt and by an asymmetrical intensity distribution within the passbands were shown to be insignificant.

4. Interstellar extinction.

An interstellar extinction curve for a reddened star can be derived by subtracting the magnitudes of an unreddened star of the same spectral type and luminosity class. Divan (1971) discussed the importance of accurate spectral type matching to derive the extinction curve in the ultraviolet. Several criteria are used to match a (nearly) unreddened star to a reddened star:

- MK classification,
- line strengths (e.g. Hβ, Hγ indices),
- size of the Balmer jump.

Of these, only the first two criteria can be determined independently of interstellar extinction effects. The Balmer jump is derived from a photometric color index and therefore can, in principle, not be separated from extinction law discontinuities and anomalies. Nevertheless, for B and A stars the Balmer jump provides a useful addition to, and check on, MK classification. Note, in this respect, that the observations at 378.5 nm are sensitive to the strength of hydrogen lines and thus allow discrimination between supergiants and dwarfs. Actual selection of matching unreddened stars was primarily based upon MK classification and line strength. The photometric data on the Balmer discontinuity served as a secondary criterion to eliminate stars with apparently wrong MK classification.

For almost all stars, MK classifications were available from the literature. To supplement published β and γ indices, these were measured for a number of stars during, as well as for several nights before, this observing run. Since these indices have not been reduced to a standard system, they are not listed here.

Matching star pairs are given in Table 5, with footnotes for some of the stars or star pairs. Note that some unreddened stars have a known (generally small) variability in magnitude (indicated with "v" in Tab. 1b). No variability in color indices has been found from the present observations and therefore these stars have not been excluded as unreddened reference stars. Calculation of the individual extinction curves then proceeded as follows.

(a) A provisional calculation of extinction curves was made by matching each reddened star with one unreddened star. From the results, a provisional average interstellar extinction curve was derived.

(b) From each set of unreddened stars (relating to one reddened star, see Tab. 5) one was selected as the 'base' (denoted star 'A'), generally the star with the least residual reddening, or in some cases the one with the most complete wavelength coverage. For any other 'unreddened' star ('B') in the same set the following magnitude relation was assumed:

$$m_B(\lambda) = m_A(\lambda) + R \cdot E(\lambda) + C$$

where $E(\lambda)$ is the provisional extinction curve and R, C are constants to be found from a least squares fit. Using this relation, all stars in each set were de-reddened to a common base.

(c) An average unreddened comparison star was then calculated for each reddened star and the actual extinction curves derived.

The resulting extinction curves have been normalized to:

$$m = 0.0 \text{ at } \lambda^{-1} = 1.50\ \mu^{-1}$$

and:

$$m = 1.0 \text{ at } \lambda^{-1} = 2.20\ \mu^{-1}$$

by making a linear fit through the points at 440 through 787 nm. The color excess $m_{2.2} - m_{1.5}$ is listed in Table 5 and plotted against E_{B-V} in Figure 2(a, b). The normalized extinction curves are given in Table 6. Only about half of the observed unreddened stars have in fact been used in the actual calculation of the extinction curves. The reason for measuring such a large set of unreddened candidates was to have the possibility of interpolation between spectral types if no satisfactory direct match could be made.

The internal accuracy of the extinction curves is determined by the accuracy of the individual stellar magnitudes (Tab. 3). The external accuracy of the extinction curves is dominated by errors of mismatch. There is no uniform way to calculate the magnitude of this type of error. The influence of an error on interpretation depends on the type of information which one tries to extract from the curves; e.g., change in slope at 2.3 μ^{-1} *versus* broadband feature at 1.8 μ^{-1}. The most prominent effect for the B to F stars occurs in the UV, because of the Balmer jump. An analysis of the magnitude of this error will be presented in the next section. Note that the disturbing features within the passbands, as listed in Table 2, will not enter the extinction curves, as they cancel out by the matching process.

5. Analysis and discussion.

5.1. Curve representation; broadband features.

Figure 3 shows the mean normalized interstellar extinction curve, which is a weighted average over all 19 stars. The data are included in Table 6 (last column). The weight of each star is taken equal to the color excess, $m_{2.2} - m_{1.5}$. Error bars indicate standard deviation (not mean error) to illustrate the spread in individual extinction curves. Error bars are larger in the UV because of the difference in slope for each individual star in this wavelength region. The relatively large deviation at $\lambda^{-1} = 1.270\ \mu^{-1}$ is at least partly attributable to a decrease in photometric accuracy.

Two main extinction features are immediately evident: the change in slope in the ultraviolet, and the dip around 1.8 μ^{-1}. To bring out details more clearly, previous investigators (Hayes *et al.* 1973; Rex 1974; Van Breda *et al.* 1981) fitted a simple and smooth theoretical curve to the data and presented the residuals of extinction *versus* this theoretical curve. A danger in this approach is that small features in the $2.0 - 2.5\ \mu^{-1}$ range will influence the curve fitting process and may even be absorbed by it. A simpler method to obtain residuals (which is also less dependent on theoretical assumptions) is to subtract a straight line approximation.

Figure 4(a) shows residuals for the average extinction after subtraction of a straight line passing through the normalization points. Error bars again represent standard deviation of the individual curves from the mean (as in Fig. 2).

Figure 4(b) shows residuals for two individual curves: HD 73882 and HD 112272. The stars are selected for their widely different strength of the 1.8 μ^{-1} feature. The accuracy of these individual curves is determined by 3 elements:

- accuracy of reddened star observations,
- accuracy of unreddened star observations,
- accuracy of spectral type matching.

The combined effect of observational accuracy for unreddened stars and of spectral type matching can be assessed by checking the deviations of the individual unreddened stars from the calculated average. For the unreddened average used with HD 112272, the mean standard deviation averaged over all wavelengths is 0.004, with a maximum of 0.006 for $\lambda^{-1} < 2.7\ \mu^{-1}$. The standard deviation goes up to 0.016 only for the three points at $\lambda^{-1} = 2.939$, 2.863 and 2.778 μ^{-1}, apparently because of inadequate matching. The observational accuracy of the individual unreddened stars is of the same order (around 0.005). For the unreddened average used with HD 73882 the mean standard deviation is 0.006 with a maximum of 0.010 at both ends of the wavelength scale. The observational accuracy of the individual unreddened stars is also around 0.006. It therefore seems justified to assume an overall accuracy for the individual extinction curves of 0.006, which is indicated by a single error bar in Figure 4(b). Individual error bars are shown only where the observational accuracy of HD 73882 or HD 112272 is worse than 0.006, or where the average unreddened star has a mean error $(= \text{st. dev.}/\sqrt{n}) > 0.006$. Figure 4(b) thus demonstrates that extinction features exist which are different from star to star. This confirms the results of Rex (1974) and Van Breda *et al.* (1981), which were obtained with a closer spacing of wavelength points. The present results are free of the uncertainty in the extinction curves obtained by the above two authors resulting from polarization effects in the grating.

5.2. Influence of known diffuse bands.

An extensive list of diffuse interstellar bands has been published by Herbig (1975). The expected effects of these bands within the filter passbands have been estimated. It was assumed for simplicity that the equivalent widths as given for HD 183143 ($E_{B-V} = 1.3$) by Herbig are typical values and are proportional to the extinction value. Diffuse band effects are then to be expected at only three wavelengths. For unit reddening ($m_{2.2} - m_{1.5} = 1$, corresponding to $E_{B-V} = 0.7$) the calculated magnitude effects are:

$$0.009 \text{ at } \lambda^{-1} = 2.275\ \mu^{-1},$$
$$0.004 \text{ at } \lambda^{-1} = 1.849\ \mu^{-1},$$
$$0.009 \text{ at } \lambda^{-1} = 1.718\ \mu^{-1}.$$

All other filters have diffuse band effects less than 0.002 magnitudes. Corrected magnitudes are indicated in Figure 4(a).

5.3. The ultraviolet extinction gradient.

The UV extinction gradient $k_u = \mathrm{d(ext)/d}\,(\lambda^{-1})$ is defined by drawing a straight line through the six points at 2.385 through 2.939 μ^{-1}. Calculated values based on the normalized extinction curves can be found in Table 5. There is a considerable spread in k_u values, and one may wonder how much of it is real and how much is caused by insufficient matching of spectral types. To assess the possible magnitude of a matching error, a comparison is made with the slope of the UV extinction curve using only two wavelength points. These points (at $\lambda^{-1} = 2.385$ and 2.476 μ^{-1}) are chosen to avoid the extinction 'knee' at 2.3 μ^{-1} and the Balmer discontinuity starting around 2.6 μ^{-1} and are virtually unaffected by these two effects. The resulting slope, k_b, is plotted against k_u in Figure 5. Bad matching would lead to an increase in spread of k_u, not in spread of k_b. The statistical relation between k_u and k_b is such that no definite conclusions can be drawn.

A plot of k_u *versus* color excess is shown in Figure 6. There is an apparent spread in k_u which is larger for stars with smaller color excess values. This effect would be expected if the interstellar extinction is due to a superposition of many clouds with different particle size mixes. The less extinction, the fewer clouds there will be along the line of sight, and the larger the fractional deviations from the average k_u that can be expected. In addition, small errors (e.g. of matching) scale inversely proportional to the total color excess because of the normalization process.

The plot of k_u *versus* spectral type (Fig. 7a) suggests that there is a relation between the two. Several possible causes are:

(a) A real dependence on spectral type:

This would imply that a sizeable part of the observed extinction can be attributed to particles which are more or less 'local' to the star being observed. The correlation (Fig. 7a) is such that hotter stars show higher k_u which, in terms of particle sizes, indicates smaller particles. The effective particle size could then either be local to the star itself, or be indicative of the more general characteristics of the regions in which hot stars tend to be situated.

(b) A systematic matching error, which is spectral type dependent:

An analysis of the remaining spread of the points around the linear regression line in Figure 5, shows that a matching error can indeed cause k_u to be off by 0.1. The Balmer jump is most notable for B stars. One expects the k_u for O stars to be unaffected so that k_u is systematically too small for B stars (see Fig. 7a). A plot of k_b *versus* spectral type would show this effect, if at all, to a much lesser extent. As shown in Figure 7b, the effect is, if anything, stronger.

(c) Statistics may be fooling us:

This seems the most plausible explanation for the moment.

It is interesting to compare the ultraviolet extinction gradient with results obtained by other authors. Ardeberg *et al.* (1982) determined the ultraviolet gradient, relative to the red/visual, to be about 0.78, i.e. equivalent to $k_u = 1.11$ when using the present normalization. Their result is based mainly on a sample of O type stars, with a median spectral type 07.5. Whittet *et al.* (1973) have determined extinction curves for a number of stars of spectral types B and later and find a range of UV slopes which is considerably wider than the range presented in this article. Interestingly, their range narrows when more accurate spectral type matching is applied (Whittet *et al.* 1976). Their groups A and B are approximately represented by $k_u = 0.8$ to 1.0. Thus, for B type stars they find $k_u < 1$. When plotted *versus* spectral type (Fig. 7a) the results from Ardeberg & Whittet seem at least consistent with the present result in terms of spectral type dependency.

A final cause for the spread in the UV extinction gradient (Tab. 5) may be a local variation in the reddening law. From the foregoing analysis it is tentatively concluded that this is the case. Such a local variation is then also to be expected for interstellar polarization curves. A discussion of extinction features for individual stars in relation to their polarization curves is in preparation.

Acknowledgements.

Dr. J.M. Greenberg and dr. J. Tinbergen instigated and stimulated the observational program of which the present investigation is a part. This research would not have been completed without their continuous advice and encouragement.

References

Ardeberg A., Virdefors B. 1982, A&A 115, 347
Breger M. 1976, ApJS 32, 1
Divan L. 1971, A&A 12, 76
Hayes D.S., Mavko G.E., Radick R.R., Rex K.H., Greenberg J.M. 1973, in Interst. Dust and Related Topics, IAU Symp. 54 J.M. Greenberg and H.C. van de Hulst Eds. (Reidel, Dordrecht, Boston) p. 83
Herbig G.H. 1975, ApJ 196, 129
Jaschek C., Conde H., de Sierra A.C. 1964, Publ. Obs. La Plata 28
Kennedy P.M., Buscombe W. 1974, MK Spectral Classifications, publ. Evanston
Lub J., Pel J.W. 1977, A&A 54, 137
Nicolet B. 1978, A&AS 34, 1
Rex K.H. 1974, Unpublished PhD Thesis, Rensselaer Polytechnic Institute
Tüg H. 1978, Unpublished PhD Thesis, Universität Bochum
Tüg H. 1980, A&A 82, 195
Van Breda I.G., Whittet D.C.B. 1981, MNRAS 195, 79
Whiteoak J.B. 1966, ApJ 144, 305
Whittet D.C.B., Van Breda I.G., Nandy K. 1973, Nature Phys. Sci. 243, 21
Whittet D.C.B., Van Breda I.G., Glass I.S. 1976, MNRAS 177, 625

TABLE 1a. *Reddened program stars for which an interstellar extinction curve is derived in the present article. Main sources of data were Nicolet (1978) for UBV data and the Jaschek and Kennedy compilations for MK types.*

HD	MK	V	B-V	E_{B-V}
46150	O5 V(f)	6.76	0.13	0.45
46223	O4 V(f)	7.28	0.22	0.54
47032	B0 III	8.83	0.45	0.75
47240	B1 II	6.15	0.14	0.40
47382	B0 III-IV	7.14	0.17	0.47
73699	B3 V	7.59	0.05	0.25
73882	O8 V	7.24	0.40	0.72
74180	F2 Ia	3.83	0.70	0.45
75211	O8 II(f)	7.51	0.41	0.73
75860	B1.5 Iab	7.60	0.73	0.91
80077	B2 Iape	7.65	1.30	1.47
93737	A0 Ia	6.00	0.27	0.26
93873	B0.5 Iab	7.81	0.46	0.67
111613	A1 Ia	5.75	0.38	0.35
112272	B0.5 Ia	7.46	0.83	1.05
112364	B1 Ib	7.38	0.21	0.40
148937	O6.5 fp	6.72	0.36	0.68
152246	O9 III	7.30	0.17	0.48
152408	O8 fp	5.77	0.15	0.47

TABLE 2. *Data on the filters and side band effects. Δm represents a calculated upper limit for the deviation of the observed magnitude from the true stellar continuum.*

λ_0 (nm)	λ_0^{-1} (μ^{-1})	band-width (nm)	peak trans-mission	Δ m	main features within (or near) bandpass (O, B, A stars)
340.2	2.939	4.2	0.30	0.02	atmospheric extinction
349.3	2.863	4.0	0.29	0.02	Balmer discontinuity
360.0	2.778	5.2	0.26	≤0.10	Balmer discontinuity
378.5	2.642	4.8	0.35	var	Balmer discontinuity
403.8	2.476	4.6	0.37	0.02	Hδ, Hε, HeI4026
419.2	2.385	10.4	0.59	0.01	Hδ, HeII4200
439.5	2.275	4.4	0.36	0.02	Hγ
449.6	2.224	8.4	0.59	0.02	HeI4471, HeII4541
470.8	2.124	9.6	0.61	0.04	Hβ, HeII4686 (emission for Of)
499.9	2.000	8.2	0.61	0.01	Hβ, HeI4922, HeI5015
520.5	1.921	9.4	0.61	0.01	-
540.7	1.849	10.0	0.64	0.02	HeII5415
560.1	1.785	10.4	0.60	0.01	-
582.1	1.718	9.8	0.65	0.01	HeI5876
610.7	1.637	8.4	0.56	0.01	-
640.0	1.563	11.4	0.61	0.01	Hα
668.1	1.497	8.6	0.59	0.02	Hα, HeI6678
710.2	1.408	9.2	0.57	0.01	HeI7065; blue leak filter (Δm ≤ 0.005)
750.5	1.332	7.8	0.56	0.01	-
787.3	1.270	8.0	0.56	0.01	-

TABLE 1b. *Observed stars with small reddening, including photometric standard stars. Sources of data: as for Table 1a.*

HD	MK	V	B-V	E_{B-V}
17081	B7 V	4.25	-0.14	-0.02
36486	O9.5 I	2.23v	-0.22	0.05
36512	B0 V	4.62	-0.26	0.04
36861/2	O8	3.39	-0.18	0.14
37027	B9.5 IV-V	8.07	-0.03	0.02
37043	O8.5 III	2.74	-0.25	0.06
37128	B0 Ia	1.70	-0.19	0.05
37468	O9.5 V	3.81	-0.24	0.06
37742/3	O9.5 I/B3	1.77	-0.21	0.06
38666	O9.5 IV	5.17	-0.28	0.02
38771	B0.5 Ia	2.06	-0.17	0.05
41534	B2 V	5.65	-0.19	0.05
44743	B1 II-III	1.98v	-0.23	0.03
46300	A0 Ib	4.50	0.00	-0.01
47431	B8 III(n)	6.57	-0.07	0.02
47839	O7	4.64v	-0.24	0.06
49798	O6	8.27	-0.30	0.02
51309	B3 II	4.38	-0.06	0.10
52089	B2 II	1.50	-0.21	0.02
53138	B3 Ia	3.03	-0.09	0.05
57060	O8.5 If	4.98v	-0.15	0.14
57061	O9 I	4.39	-0.16	0.05
57682	O9 V	6.43	-0.19	0.12
59864	B0 Ib	7.64	-0.09	0.15
60848	O8 Vpe	6.87	-0.20	0.12
64760	B0.5 Ib	4.24	-0.14	0.08
66811	O5 f	2.25	-0.26	0.06
70761	F2 Ia	5.90	0.37	0.12
74280	B3 V	4.30	-0.20	0.00
74575	B1.5 III	3.68	-0.18	0.07
80404	F0 I	2.25	0.18	0.01
87504	B9 III-IV	4.60	-0.09	-0.03
87737	A0 Ib	3.52	-0.03	-0.04
87901	B7 V	1.35	-0.11	0.01
90882	B9.5 V	5.21	-0.06	0.00
91316	B1 Iab	3.85	-0.14	0.05
93695	B5 V	6.47	-0.12	0.04
93943	B9.5 IV-V	5.91	0.00	0.06
100889	B9.5 V	4.70	-0.08	-0.02
104337	B1.5 V	5.28	-0.16	0.09
116003	B1 II	6.95	0.01	0.20
119608	B1 Ib	7.57	-0.07	0.12
122980	B2 V	4.36	-0.19	0.05
144470	B1 V	3.96	-0.04	0.22

TABLE 3. *Observed energy distributions of the program stars. The following data are listed: – the magnitudes m_ν relative to the Hayes-Latham calibration of Vega, – the mean observational error (M.E.), – the number of independent observations (N) (see text). Magnitudes are defined as $m_\nu = -2.5\ log\ F_\nu +$ constant, where F_ν is the flux per unit frequency interval.*

HD		WAVELENGTH (NM) 340	349	360	378	404	419	440	450	471	500	520	541	560	582	611	640	668	710	750	787
17081	MAGN	0.470	0.475	0.472	-0.025	-0.276	-0.232	-0.182	-0.154	-0.094	0.000	0.051	0.097	0.140	0.192	0.273	0.319	0.377	0.448	0.546	0.612
	M.E.	0.004	0.006	0.005	0.004	0.005	0.003	0.006	0.001	0.003	0.003	0.004	0.005	0.004	0.005	0.005	0.005	0.004	0.003	0.005	0.009
	N	5	3	3	3	3	3	3	10	3	3	3	3	3	3	2	3	2	2	2	2
36486	MAGN	-0.453	-0.411	-0.339	-0.370	-0.312	-0.259	-0.209	-0.162	-0.095	0.000	0.063	0.129	0.184	0.249	0.324	0.396	0.458	0.545	0.647	0.731
	M.E.	0.006	0.008	0.006	0.002	0.004	0.006	0.002	0.001	0.005	0.004	0.003	0.004	0.006	0.007	0.002	0.007	0.001	-	0.001	-
	N	7	5	5	5	3	5	3	15	4	4	4	5	5	5	3	5	3	1*	3	1*
36512	MAGN	-0.486	-0.442	-0.381	-0.392	-0.367	-0.303	-0.232	-0.191	-0.101	0.000	0.065	0.134	0.193	0.264	0.360	0.428	0.510	0.609	0.722	0.805
	M.E.	0.003	0.002	0.003	0.002	0.003	0.002	0.002	0.001	0.002	0.001	0.002	0.002	0.003	0.001	0.003	0.003	0.003	0.004	0.006	0.013
	N	7	5	5	5	4	5	4	13	4	4	4	4	4	4	2	4	2	2	2	2
36861	MAGN	-0.384	-0.355	-0.291	-0.317	-0.293	-0.235	-0.192	-0.145	-0.085	0.000	0.048	0.111	0.148	0.206	0.288	0.328	0.394	0.471	0.566	0.630
	M.E.	0.006	0.008	0.008	0.005	0.005	0.006	0.002	0.001	0.007	0.004	0.004	0.001	0.002	0.002	0.004	0.002	0.002	0.001	0.003	0.011
	N	7	5	5	5	3	5	3	16	4	4	4	5	5	5	4	5	4	2	4	2
37027	MAGN	1.092	1.073	1.046	0.296	-0.199	-0.173	-0.129	-0.129	-0.079	0.000	0.046	0.080	0.102	0.151	0.212	0.250	0.296	0.392	0.399	0.474
	M.E.	0.004	0.007	0.005	0.003	0.003	0.002	0.003	0.001	0.002	0.002	0.001	0.002	0.002	0.004	0.008	0.006	0.011	0.009	0.029	0.032
	N	12	8	8	8	7	8	7	27	7	7	7	10	10	10	5	10	5	5	5	5
37043	MAGN	-0.470	-0.440	-0.357	-0.381	-0.333	-0.278	-0.219	-0.172	-0.102	0.000	0.062	0.136	0.190	0.262	0.345	0.408	0.481	0.561	0.678	0.743
	M.E.	0.006	0.008	0.010	0.006	0.008	0.006	0.005	0.000	0.005	0.005	0.003	0.002	0.005	0.003	0.002	0.005	0.003	-	0.003	-
	N	7	4	4	4	3	4	3	17	5	5	5	7	7	7	3	7	3	1*	3	1*
37128	MAGN	-0.388	-0.354	-0.282	-0.341	-0.275	-0.232	-0.182	-0.145	-0.081	0.000	0.049	0.105	0.157	0.216	0.276	0.347	0.392	0.483	0.569	0.652
	M.E.	0.003	0.007	0.009	0.003	0.006	0.003	0.002	0.001	0.004	0.002	0.002	0.003	0.004	0.003	0.002	0.004	0.004	0.004	0.004	0.001
	N	7	4	4	4	3	5	4	15	6	6	6	5	5	5	4	5	4	2*	4	2*
37468	MAGN	-0.430	-0.391	-0.337	-0.361	-0.352	-0.277	-0.211	-0.183	-0.090	0.000	0.061	0.115	0.167	0.236	0.324	0.381	0.462	0.543	0.660	0.740
	M.E.	0.003	0.004	0.005	0.004	0.005	0.007	0.006	0.000	0.004	0.004	0.005	0.002	0.002	0.002	0.002	0.004	0.002	-	0.003	-
	N	7	4	4	4	3	4	3	14	5	5	5	4	4	4	3	4	3	1*	3	1*
37742	MAGN	-0.442	-0.411	-0.331	-0.364	-0.304	-0.253	-0.204	-0.160	-0.094	0.000	0.056	0.110	0.170	0.224	0.301	0.362	0.423	0.508	0.611	0.692
	M.E.	0.007	0.009	0.006	0.003	0.002	0.006	0.003	0.001	0.005	0.004	0.001	0.003	0.004	0.005	0.002	0.002	0.001	0.002	0.002	0.002
	N	7	4	4	4	3	4	3	16	5	5	5	5	5	5	4	5	4	2*	4	2*
38666	MAGN	-0.523	-0.479	-0.414	-0.417	-0.381	-0.315	-0.246	-0.198	-0.101	0.000	0.067	0.142	0.199	0.275	0.375	0.439	0.531	0.638	0.754	0.801
	M.E.	0.001	0.001	0.002	0.003	0.003	0.001	0.002	0.000	0.000	0.002	0.004	0.001	0.002	0.003	0.002	0.002	0.003	0.009	0.002	0.005
	N	5	3	3	3	2	3	2	13	3	3	3	4	4	4	4	4	4	2*	4	2*
38771	MAGN	-0.361	-0.329	-0.261	-0.331	-0.270	-0.227	-0.176	-0.143	-0.079	0.000	0.046	0.102	0.156	0.211	0.279	0.342	0.399	0.477	0.574	0.642
	M.E.	0.004	0.005	0.008	0.003	0.006	0.003	0.003	0.000	0.002	0.001	0.002	0.002	0.003	0.002	0.001	0.003	0.002	0.001	0.002	0.004
	N	8	4	4	4	3	4	3	17	6	6	6	5	5	5	4	5	4	4	4	4
41534	MAGN	-0.045	-0.011	0.024	-0.184	-0.323	-0.278	-0.205	-0.178	-0.109	0.000	0.053	0.117	0.172	0.235	0.327	0.387	0.458	0.541	0.653	0.726
	M.E.	0.002	0.002	0.002	0.003	0.003	0.002	0.002	0.001	0.002	0.002	0.002	0.002	0.004	0.002	0.004	0.003	0.005	0.005	0.008	0.011
	N	7	5	5	5	4	5	4	14	4	4	4	4	4	4	2	4	2	3	2	3
44743	MAGN	-0.340	-0.305	-0.234	-0.340	-0.340	-0.286	-0.211	-0.174	-0.100	0.000	0.062	0.130	0.193	0.260	0.351	0.417	0.488	0.577	0.684	0.750
	M.E.	0.006	0.008	0.005	0.003	0.006	0.008	0.002	0.001	0.005	0.006	0.002	0.003	0.004	0.005	0.005	0.006	0.001	0.003	0.003	0.001
	N	6	4	4	4	3	4	3	14	4	4	4	5	5	5	3	5	3	2*	3	2*
46150	MAGN	0.050	0.053	0.050	-0.010	-0.031	-0.019	-0.025	-0.023	-0.006	0.000	-0.014	0.003	-0.014	0.011	0.032	0.058	0.061	0.079	0.146	0.131
	M.E.	0.003	0.007	0.003	0.003	0.003	0.003	0.002	0.000	0.002	0.002	0.001	0.003	0.002	0.001	0.001	0.003	0.003	0.007	0.009	0.018
	N	9	6	6	6	6	6	6	20	6	6	6	7	7	7	4	7	4	3	4	2*
46223	MAGN	0.181	0.180	0.153	0.082	0.056	0.064	0.038	0.028	0.022	0.000	-0.029	-0.032	-0.058	-0.044	-0.023	-0.030	-0.028	-0.038	0.004	0.030
	M.E.	0.003	0.003	0.005	0.004	0.002	0.004	0.005	0.001	0.002	0.002	0.001	0.002	0.003	0.003	0.004	0.003	0.007	0.009	0.005	0.019
	N	9	6	6	6	6	3	3	20	4	4	4	7	7	7	4	7	4	2*	4	2*
46300	MAGN	1.091	1.063	0.963	0.024	-0.129	-0.107	-0.122	-0.078	-0.051	0.000	0.033	0.046	0.064	0.096	0.153	0.180	0.209	0.258	0.329	0.382
	M.E.	0.002	0.001	0.002	0.002	0.009	0.008	0.002	0.001	0.001	0.001	0.001	0.002	0.003	0.003	0.003	0.002	0.002	0.005	0.004	0.008
	N	2	2	2	2	2	2	2	9	2	2	2	3	3	3	4	3	4	4	4	4
47032	MAGN	0.545	0.562	0.477	0.329	0.234	0.206	0.163	0.140	0.095	0.000	-0.082	-0.135	-0.187	-0.187	-0.200	-0.252	-0.245	-0.304	-0.298	-0.243
	M.E.	0.007	0.008	0.005	0.004	0.003	0.003	0.004	0.001	0.003	0.003	0.004	0.005	0.004	0.004	0.006	0.006	0.009	0.025	0.015	0.097
	N	12	7	7	7	7	6	6	26	8	8	8	10	10	10	4	9	4	2*	4	2*
47240	MAGN	0.200	0.193	0.193	0.018	-0.012	-0.012	-0.010	-0.014	0.003	0.000	-0.014	-0.009	-0.013	0.009	0.032	0.047	0.068	0.067	0.137	0.139
	M.E.	0.002	0.004	0.004	0.004	0.004	0.003	0.002	0.001	0.003	0.001	0.001	0.001	0.003	0.003	0.004	0.002	0.004	0.007	0.008	0.001
	N	7	5	5	5	5	5	5	16	4	4	4	5	5	5	4	5	4	2*	4	2*
47382	MAGN	0.151	0.147	0.143	0.022	-0.018	-0.010	-0.004	-0.010	0.006	0.000	-0.024	-0.029	-0.043	-0.019	0.007	0.015	0.034	0.046	0.102	0.071
	M.E.	0.002	0.002	0.004	0.002	0.002	0.004	0.003	0.001	0.001	0.003	0.001	0.004	0.003	0.003	0.004	0.003	0.006	0.010	0.006	0.041
	N	13	6	6	6	6	4	4	20	5	5	5	7	7	7	4	7	4	2*	5	2*
47431	MAGN	0.696	0.701	0.670	0.032	-0.238	-0.199	-0.156	-0.137	-0.084	0.000	0.047	0.075	0.108	0.154	0.229	0.271	0.313	0.382	0.477	0.497
	M.E.	0.005	0.001	0.012	0.000	0.004	-	-	0.001	0.003	0.002	0.000	0.002	0.001	0.002	0.003	0.003	0.003	0.009	0.010	0.006
	N	4	2	2	2	2	1*	1*	13	2	2	2	6	6	6	3	6	3	2*	3	2*
47839	MAGN	-0.471	-0.428	-0.369	-0.382	-0.342	-0.282	-0.225	-0.182	-0.099	0.000	0.060	0.132	0.179	0.253	0.342	0.396	0.476	0.571	0.682	0.764
	M.E.	0.002	0.003	0.001	0.002	0.003	0.003	0.007	0.001	0.002	0.001	0.002	0.004	0.003	0.002	0.001	0.003	0.001	0.001	0.001	0.006
	N	6	4	4	4	4	3	2	16	3	3	3	6	6	6	3	6	3	3	3	3
49798	MAGN	-0.619	-0.569	-0.509	-0.474	-0.381	-0.306	-0.249	-0.194	-0.097	0.000	0.071	0.155	0.195	0.271	0.385	0.443	0.519	0.627	0.806	0.808
	M.E.	0.002	0.003	0.002	0.004	0.003	0.005	0.004	0.001	0.001	0.003	0.003	0.007	0.003	0.005	0.010	0.009	0.014	-	0.043	-
	N	5	3	3	3	3	2	2	11	3	3	3	4	4	4	2	4	2	1*	2	1*
51309	MAGN	0.138	0.147	0.154	-0.158	-0.202	-0.162	-0.135	-0.114	-0.065	0.000	0.026	0.058	0.089	0.136	0.189	0.233	0.280	0.329	0.409	0.462
	M.E.	0.002	0.005	0.004	0.002	0.002	0.001	0.001	0.000	0.002	0.002	0.002	0.001	0.001	0.001	0.003	0.003	0.003	0.002	0.002	0.004
	N	6	4	4	4	4	4	4	14	3	3	3	4	4	4	4	4	4	2*	4	2*
52089	MAGN	-0.281	-0.248	-0.187	-0.320	-0.312	-0.266	-0.206	-0.167	-0.097	0.000	0.055	0.111	0.177	0.238	0.320	0.380	0.446	0.523	0.634	0.701
	M.E.	0.005	0.007	0.006	0.003	0.004	0.004	0.003	0.000	0.004	0.005	0.005	0.002	0.002	0.002	0.007	0.005	0.000	-	0.005	-
	N	5	5	5	5	4	5	4	14	5	5	5	4	4	4	2	4	2	1*	2	1*
53138	MAGN	0.000	0.015	0.025	-0.222	-0.217	-0.176	-0.151	-0.123	-0.073	0.000	0.024	0.062	0.099	0.142	0.202	0.247	0.296	0.350	0.437	0.491
	M.E.	0.004	0.004	0.003	0.003	0.002	0.002	0.003	0.000	0.002	0.000	0.003	0.001	0.001	0.002	0.005	0.002	0.001	0.008	0.002	0.007
	N	7	5	5	5	4	4	3	15	3	3	3	4	4	4	3	4	3	2	3	2
57060	MAGN	-0.367	-0.332	-0.298	-0.318	-0.256	-0.210	-0.173	-0.140	-0.106	0.000	0.044	0.097	0.130	0.185	0.253	0.289	0.336	0.411	0.505	0.554
	M.E.	0.003	0.002	0.003	0.005	0.002	0.000	0.005	0.000	0.002	0.002	0.002	0.002	0.002	0.003	0.003	0.005	0.003	0.003	0.005	0.005
	N	6	3	3	3	2	3	2	18	4	4	4	6	6	6	4	6	4	4	4	4
57061	MAGN	-0.369	-0.343	-0.295	-0.322	-0.280	-0.230	-0.182	-0.149	-0.083	0.000	0.048	0.095	0.136	0.191	0.272	0.308	0.369	0.453	0.551	0.607
	M.E.	0.003	0.008	0.006	0.006	0.003	0.001	0.008	0.001	0.003	0.004	0.004	0.003	0.003	0.004	0.003	0.005	0.005	0.001	0.001	0.009
	N	6	3	3	3	2	4	3	14	5	5	5	4	4	4	3	4	3	2*	3	2*
57682	MAGN	-0.396	-0.361	-0.307	-0.324	-0.296	-0.242	-0.193	-0.154	-0.083	0.000	0.048	0.110	0.153	0.218	0.297	0.353	0.421	0.501	0.580	0.622
	M.E.	0.001	0.002	0.002	0.001	0.005	0.003	0.005	0.001	0.003	0.002	0.003	0.002	0.004	0.002	0.003	0.004	0.002	0.007	0.012	0.021
	N	7	4	4	4	3	4	3	19	4	4	4	7	7	7	3	7	3	3	3	3

TABLE 3. *(continued)*

HD		WAVELENGTH (NM) 340	349	360	378	404	419	440	450	471	500	520	541	560	582	611	640	668	710	750	787
59864	MAGN	-0.078	-0.058	-0.022	-0.174	-0.218	-0.180	-0.142	-0.123	-0.072	0.000	0.034	0.078	0.117	0.171	0.234	0.279	0.336	0.382	0.477	0.506
	M.E.	0.003	0.004	0.003	0.002	0.002	0.002	0.002	0.001	0.002	0.002	0.002	0.003	0.003	0.004	0.004	0.003	0.004	0.018	0.030	0.057
	N	9	6	6	6	6	5	5	21	4	4	4	8	8	8	4	8	4	2*	4	2*
60848	MAGN	-0.444	-0.428	-0.383	-0.381	-0.317	-0.252	-0.199	-0.159	-0.078	0.000	0.065	0.121	0.164	0.217	0.311	0.354	0.379	0.428	0.588	0.602
	M.E.	0.002	-	-	-	-	-	-	0.002	0.005	0.003	0.004	0.002	0.002	0.002	0.002	0.002	0.006	0.005	0.017	0.013
	N	4	1*	1*	1*	1*	1*	1*	13	3*	3*	3*	7	7	7	2*	7	2*	2*	2*	2*
64760	MAGN	-0.307	-0.275	-0.233	-0.305	-0.270	-0.223	-0.174	-0.144	-0.072	0.000	0.041	0.092	0.137	0.191	0.258	0.310	0.373	0.443	0.536	0.603
	M.E.	0.002	0.004	0.002	0.004	0.002	0.001	0.001	0.000	0.002	0.002	0.003	0.003	0.003	0.003	0.005	0.003	0.002	0.004	0.004	0.004
	N	6	4	4	4	3	4	3	15	3	3	3	4	4	4	3	4	3	3	3	3
66811	MAGN	-0.561	-0.511	-0.470	-0.451	-0.365	-0.286	-0.239	-0.199	-0.158	0.000	0.059	0.130	0.187	0.247	0.339	0.401	0.463	0.531	0.667	0.746
	M.E.	0.007	0.002	0.002	0.002	0.000	0.003	0.002	0.001	0.000	0.004	0.003	0.001	0.003	0.004	0.003	0.004	0.002	0.007	0.002	0.005
	N	5	3	3	3	3	3	3	16	2	2	2	7	7	7	3	7	3	2	3	2
70761	MAGN	2.281	2.214	1.928	0.609	0.206	0.184	0.152	0.104	0.008	0.000	0.009	-0.034	-0.082	-0.108	-0.095	-0.119	-0.140	-0.137	-0.125	-0.130
	M.E.	0.013	0.015	0.007	0.003	0.005	0.007	0.010	0.001	0.000	0.004	0.006	0.003	0.006	0.007	0.001	0.005	0.008	-	0.009	-
	N	2	2	2	2	2	2	2	8	2	2	2	3	3	3	3	3	3	1*	3	1*
73699	MAGN	0.189	0.196	0.205	0.021	-0.115	-0.107	-0.074	-0.072	-0.043	0.000	-0.004	0.014	0.021	0.056	0.097	0.126	0.142	0.189	0.224	0.397
	M.E.	0.003	0.003	0.002	0.002	0.002	0.002	0.001	0.001	0.002	0.001	0.001	0.002	0.003	0.002	0.003	0.004	0.009	0.031	0.006	0.115
	N	12	8	8	8	7	6	5	26	5	5	5	8	8	8	4	8	4	2*	4	2*
73882	MAGN	0.569	0.532	0.500	0.345	0.212	0.179	0.120	0.096	0.060	0.000	-0.060	-0.100	-0.151	-0.172	-0.195	-0.247	-0.284	-0.327	-0.336	-0.363
	M.E.	0.003	0.003	0.002	0.002	0.003	0.002	0.001	0.001	0.001	0.002	0.002	0.002	0.001	0.003	0.007	0.003	0.001	0.011	0.008	0.035
	N	13	10	9	9	7	8	6	26	5	5	5	8	8	8	4	8	4	2*	4	2*
74180	MAGN	2.685	2.571	2.222	0.921	0.545	0.478	0.406	0.306	0.115	0.000	-0.049	-0.164	-0.248	-0.311	-0.350	-0.425	-0.493	-0.573	-0.600	-0.658
	M.E.	0.005	0.001	0.005	0.001	0.001	0.001	0.002	0.001	0.003	0.002	0.003	0.001	0.001	0.002	0.001	0.003	0.001	0.000	0.001	0.004
	N	3	3	3	3	3	3	3	10	3	3	3	3	3	3	4	3	4	2*	4	2*
74280	MAGN	-0.014	0.011	0.038	-0.193	-0.323	-0.270	-0.208	-0.174	-0.101	0.000	0.060	0.117	0.171	0.233	0.323	0.382	0.449	0.529	0.641	0.708
	M.E.	0.002	0.001	0.004	0.001	0.000	0.002	0.001	0.000	0.002	0.001	0.005	0.002	0.001	0.001	0.004	0.001	0.003	0.002	0.004	0.001
	N	4	3	3	3	3	3	3	14	2	2	2	5	5	5	3	5	3	3	3	3
74575	MAGN	-0.201	-0.170	-0.129	-0.277	-0.384	-0.255	-0.194	-0.166	-0.094	0.000	0.046	0.100	0.152	0.213	0.294	0.350	0.422	0.496	0.607	0.670
	M.E.	0.003	0.002	0.003	0.003	0.003	0.003	0.004	0.001	0.002	0.003	0.002	0.003	0.002	0.003	0.003	0.003	0.006	0.004	0.006	0.006
	N	7	5	5	5	5	5	4	14	4	4	4	4	4	4	2	4	2	3	2	3
75211	MAGN	0.488	0.458	0.420	0.285	0.195	0.168	0.108	0.097	0.049	0.000	-0.064	-0.105	-0.160	-0.179	-0.191	-0.224	-0.239	-0.241	-0.257	-0.241
	M.E.	0.002	0.003	0.003	0.003	0.001	0.002	0.004	0.001	0.003	0.004	0.003	0.004	0.003	0.002	0.003	0.005	0.003	0.008	0.006	0.027
	N	13	10	10	10	8	8	6	27	5	5	5	8	8	8	4	8	4	2*	4	2*
75860	MAGN	1.073	1.006	0.925	0.639	0.494	0.416	0.320	0.235	0.145	0.000	-0.138	-0.249	-0.367	-0.438	-0.517	-0.597	-0.668	-0.805	-0.845	-0.936
	M.E.	0.004	0.006	0.003	0.003	0.004	0.003	0.004	0.001	0.002	0.003	0.002	0.002	0.003	0.002	0.006	0.006	0.003	0.006	0.006	0.056
	N	12	9	9	9	7	7	5	26	5	5	5	8	8	8	4	8	4	2*	4	2*
80077	MAGN	2.012	1.861	1.682	1.321	1.061	0.902	0.672	0.533	0.321	0.000	-0.266	-0.491	-0.687	-0.851	-1.039	-1.208	-1.397	-1.641	-1.810	-2.020
	M.E.	0.005	0.003	0.008	0.006	0.001	0.003	0.002	0.001	0.005	0.004	0.003	0.002	0.003	0.002	0.006	0.003	0.003	0.007	0.006	0.045
	N	13	8	8	8	6	6	4	26	6	6	6	8	8	8	4	8	4	2*	4	2*
80404	MAGN	1.967	1.917	1.783	0.441	0.025	0.012	0.026	0.004	-0.030	0.000	0.026	0.036	0.037	0.043	0.068	0.087	0.082	0.099	0.154	0.168
	M.E.	-	-	-	-	-	-	-	0.001	-	-	-	0.002	0.002	0.002	0.009	0.001	0.001	0.000	0.001	0.003
	N	1*	1*	1*	1*	1*	1*	1*	8	1*	1*	1*	3	3	3	4	3	4	2*	4	2*
87504	MAGN	0.765	0.763	0.742	0.097	-0.252	-0.213	-0.170	-0.148	-0.084	0.000	0.046	0.090	0.130	0.178	0.258	0.299	0.354	0.420	0.515	0.583
	M.E.	0.003	0.004	0.003	0.002	0.005	0.003	0.003	0.001	0.004	0.003	0.003	0.004	0.003	0.004	0.003	0.004	0.005	0.004	0.006	0.010
	N	7	5	5	5	4	5	4	14	4	4	4	4	4	4	2	4	2	3	2	3
87737	MAGN	0.999	0.975	0.912	-0.027	-0.168	-0.142	-0.121	-0.085	-0.072	0.000	0.039	0.068	0.090	0.128	0.189	0.220	0.257	0.306	0.388	0.431
	M.E.	0.007	0.009	0.020	0.005	0.000	0.011	0.004	0.001	0.010	0.007	0.014	0.002	0.001	0.002	0.001	0.002	0.001	-	0.000	-
	N	2*	2*	2*	2*	2*	2*	2*	8	2*	2*	2*	4	4	4	2	4	2	1*	2	1*
87901	MAGN	0.603	0.599	0.614	0.004	-0.252	-0.215	-0.165	-0.140	-0.083	0.000	0.047	0.097	0.143	0.195	0.261	0.317	0.360	0.422	0.524	0.579
	M.E.	0.005	0.313	0.008	0.002	0.006	0.004	0.002	0.000	0.004	0.002	0.002	0.002	0.002	0.003	0.003	0.004	0.003	-	0.005	-
	N	9	2	2	2	2	2	2	18	8	8	8	7	7	7	3	7	3	1*	3	1*
90882	MAGN	1.028	1.015	0.974	0.245	-0.229	-0.196	-0.150	-0.134	-0.084	0.000	0.047	0.090	0.129	0.176	0.251	0.290	0.342	0.412	0.501	0.541
	M.E.	0.004	0.001	0.005	0.004	0.005	0.002	0.002	0.000	0.002	0.004	0.002	0.002	0.003	0.003	0.001	0.002	0.004	0.001	0.007	0.028
	N	5	3	3	3	2	3	2	14	3	3	3	4	4	4	3	4	3	2*	3	2*
91316	MAGN	-0.258	-0.236	-0.204	-0.304	-0.267	-0.227	-0.179	-0.150	-0.081	0.000	0.036	0.084	0.130	0.185	0.267	0.311	0.381	0.441	0.547	0.615
	M.E.	0.004	0.003	0.002	0.002	0.000	0.002	0.005	0.000	0.001	0.003	0.001	0.001	0.003	0.004	0.002	0.001	0.002	-	0.004	-
	N	6	3	3	3	2	3	2	12	4	4	4	3	3	3	2	3	2	1*	2	1*
93695	MAGN	0.200	0.215	0.236	-0.077	-0.267	-0.231	-0.172	-0.148	-0.091	0.000	0.046	0.100	0.149	0.204	0.278	0.329	0.395	0.466	0.563	0.679
	M.E.	0.001	0.002	0.002	0.001	0.006	0.002	0.004	0.001	0.001	0.001	0.003	0.002	0.002	0.002	0.002	0.004	0.008	0.009	0.004	0.016
	N	8	5	5	5	3	5	3	21	5	5	5	8	8	8	3	8	3	3	3	4
93737	MAGN	0.977	0.921	0.832	0.197	0.089	0.081	0.044	0.041	0.010	0.000	-0.023	-0.050	-0.074	-0.076	-0.078	-0.082	-0.096	-0.100	-0.079	-0.042
	M.E.	0.003	0.003	0.006	0.001	0.004	0.002	0.002	0.000	0.001	0.003	0.002	0.001	0.002	0.001	0.003	0.003	0.003	0.003	0.002	0.002
	N	7	5	5	5	4	5	4	18	5	5	5	5	5	5	4	5	4	2*	4	2*
93873	MAGN	0.574	0.536	0.498	0.310	0.231	0.207	0.155	0.126	0.088	0.000	-0.091	-0.138	-0.178	-0.202	-0.235	-0.275	-0.314	-0.403	-0.392	-0.326
	M.E.	0.003	0.006	0.004	0.002	0.003	0.002	0.002	0.001	0.002	0.004	0.003	0.003	0.005	0.003	0.005	0.004	0.006	0.011	0.011	0.002
	N	10	6	6	6	4	6	4	24	6	6	6	8	8	8	4	8	4	2*	4	2*
93943	MAGN	1.131	1.111	1.063	0.306	-0.179	-0.163	-0.126	-0.119	-0.070	0.000	0.036	0.066	0.094	0.134	0.200	0.232	0.287	0.338	0.416	0.475
	M.E.	0.003	0.004	0.004	0.002	0.003	0.003	0.001	0.001	0.003	0.004	0.003	0.001	0.002	0.002	0.004	0.002	0.001	0.006	0.001	0.012
	N	6	4	4	4	3	3	2*	16	2	2	2	5	5	5	3	5	3	2*	3	2*
100889	MAGN	0.928	0.917	0.885	0.177	-0.240	-0.207	-0.163	-0.143	-0.089	0.000	0.050	0.089	0.126	0.175	0.252	0.295	0.351	0.424	0.508	0.580
	M.E.	0.002	0.002	0.004	0.002	0.002	0.003	0.002	0.000	0.001	0.001	0.002	0.001	0.002	0.001	0.001	0.002	0.000	-	0.004	-
	N	7	4	4	4	4	3	3	15	5	5	5	5	5	5	2*	5	2*	1*	2*	1*
104337	MAGN	-0.187	-0.155	-0.114	-0.268	-0.321	-0.269	-0.203	-0.175	-0.100	0.000	0.053	0.113	0.167	0.232	0.321	0.379	0.450	0.535	0.647	0.721
	M.E.	0.002	0.002	0.003	0.002	0.003	0.002	0.002	0.000	0.002	0.002	0.002	0.002	0.003	0.002	0.003	0.004	0.006	0.004	0.008	0.011
	N	7	5	5	5	4	5	4	14	4	4	4	4	4	4	2	4	2	3	2	3
111613	MAGN	1.426	1.347	1.204	0.342	0.185	0.162	0.112	0.095	0.035	0.000	-0.054	-0.115	-0.166	-0.181	-0.193	-0.203	-0.236	-0.252	-0.244	-0.243
	M.E.	0.004	0.004	0.002	0.003	0.004	0.001	0.001	0.000	0.001	0.004	0.002	0.001	0.002	0.002	-	0.003	-	0.003	-	0.008
	N	6	4	4	4	3	4	3	14	4	4	4	5	5	5	1*	5	1*	2*	1*	2*
112272	MAGN	1.092	1.008	0.912	0.652	0.509	0.429	0.331	0.285	0.187	0.000	-0.170	-0.286	-0.403	-0.458	-0.526	-0.597	-0.674	-0.782	-0.827	-0.878
	M.E.	0.003	0.002	0.002	0.007	0.002	0.002	0.000	0.001	0.002	0.003	0.003	0.003	0.003	0.001	0.008	0.004	0.000	0.015	0.003	0.036
	N	7	3	3	3	2*	3	2*	17	6	6	6	6	6	6	2*	6	2*	2*	2*	2*
112364	MAGN	0.242	0.231	0.238	0.078	0.019	0.019	0.024	0.014	0.018	0.000	-0.031	-0.034	-0.049	-0.029	-0.024	-0.022	-0.008	-0.012	0.015	0.000
	M.E.	0.003	0.004	0.003	0.002	0.005	0.003	0.001	0.001	0.002	0.002	0.000	0.003	0.003	0.002	-	0.006	-	0.005	-	0.024
	N	7	5	5	5	4	3	2	17	4	4	4	7	7	7	1*	7	1*	2*	1*	2*

TABLE 3. *(continued)*

HD		WAVELENGTH (NM) 340	349	360	378	404	419	440	450	471	500	520	541	560	582	611	640	668	710	750	787
116003	MAGN	-0.039	-0.025	0.005	-0.132	-0.146	-0.122		-0.084	-0.040	0.000	0.012	0.030	0.052	0.094		0.177		0.263		0.447
	M.E.	0.004	0.006	0.005	0.002	0.002	-		0.001	0.003	0.001	0.007	0.002	0.003	0.002		0.006		0.012		0.014
	N	5	3	3	3	2	1*		13	2	2	2	6	6	6		6		2*		2*
119608	MAGN	-0.091	-0.076	-0.058	-0.198	-0.191	-0.167	-0.138	-0.115	-0.061	0.000	0.024	0.057	0.090	0.136		0.244		0.346		0.461
	M.E.	0.002	0.008	0.008	0.003	-	0.002	-	0.001	0.001	0.002	0.002	0.002	0.002	0.002		0.003		0.006		0.069
	N	5	2	2	2	1*	2	1*	15	4	4	4	8	8	8		8		2*		2*
122980	MAGN	-0.096	-0.067	-0.031	-0.195	-0.332	-0.284	-0.211	-0.180	-0.107	0.000	0.056	0.117	0.172	0.237	0.330	0.387	0.467	0.547	0.666	0.738
	M.E.	0.003	0.003	0.002	0.002	0.003	0.002	0.002	0.001	0.002	0.002	0.002	0.002	0.002	0.002	0.005	0.003	0.004	0.006	0.008	0.014
	N	6	4	4	4	3	4	3	13	4	4	4	4	4	4	2	4	2	2	2	2
144470	MAGN	-0.042	-0.026	0.005	-0.106	-0.180	-0.154	-0.111	-0.099	-0.053	0.000	0.024	0.056	0.083	0.127	0.188	0.219	0.271	0.321	0.404	0.459
	M.E.	0.002	0.002	0.002	0.003	0.002	0.003	0.005	0.001	0.004	0.002	0.002	0.003	0.004	0.003	0.003	0.004	0.002	0.005	0.005	0.008
	N	5	3	3	3	2	3	2	12	4	4	4	4	4	4	2	4	2	2	2	2
148937	MAGN	0.338	0.319	0.293	0.192	0.140	0.127	0.081	0.069	0.027	0.000	-0.061	-0.089	-0.138	-0.133	-0.148	-0.156	-0.194		-0.183	
	M.E.	0.004	0.001	0.004	0.003	0.001	0.000	0.002	0.001	0.004	0.005	0.006	0.001	0.003	0.001	0.000	0.003	0.004		0.015	
	N	4	3	3	3	3	2	2	12	3	3	3	6	6	6	2*	6	2*		2*	
152246	MAGN	0.110	0.104	0.112	0.026	-0.010	-0.004	-0.009	-0.008	0.007	0.000	-0.026	-0.035	-0.053	-0.028	-0.002	-0.012	0.006		0.075	
	M.E.	0.001	0.003	0.003	0.004	0.003	0.001	0.000	0.001	0.005	0.000	0.001	0.003	0.002	0.002	0.003	0.003	0.002		0.006	
	N	2	2	2	2	2	2	2	12	2	2	2	8	8	8	2*	8	2*		2*	
152408	MAGN	0.110	0.111	0.108	0.023	0.018	0.020	-0.015	-0.042	-0.090	0.000	-0.018	-0.042	-0.074	-0.078	-0.049	-0.079	-0.125		-0.022	
	M.E.	0.006	0.003	0.007	0.001	0.001	0.004	0.002	0.000	0.003	0.005	0.006	0.002	0.002	0.004	-	0.003	-		-	
	N	2	2	2	2	2	2	2	7	2	2	2	4	4	4	1*	4	1*		1*	

An asterisk (*) indicates results which are based on observations of only one night.

TABLE 4. *Comparison of observations to standard systems. σ_{MB}, σ_{HT} are rms deviations of present data versus those of Breger, resp. Tüg. Δm_{PB-HT} is the zeropoint shift required to convert the present data (Tab. 3) to Tüg's system of absolute standards. See text for stars used in the calculation of Δm_{PB-HT}.*

λ(nm)	σ_{MB}	σ_{HT}	Δm_{PB-HT}
340	0.013	0.016	0.169
349	0.016	0.024	0.170
360	0.015	0.027	0.194
378	-	-	-
404	0.008	0.029	0.160
419	0.006	0.006	0.159
440	0.007	0.012	0.151
450	0.010	0.010	0.152
471	0.011	0.005	0.148
500	0 (def)	0.005	0.154
520	0.007	0.016	0.155
541	0.008	0.022	0.150
560	0.010	0.019	0.151
582	0.012	0.017	0.152
611	0.008	0.022	0.160
640	0.003	0.013	0.146
668	0.001	0.019	0.135
710	0.011	0.012	0.119
750	0.001	0.019	0.137
787	0.021	0.017	0.132

TABLE 5. *Star pairs for extinction calculation, and resulting extinction parameters.*

reddened star	matching 'unreddened' star	see note	resulting color excess ($m_{2.2}$-$m_{1.5}$)	UV gradient k_u
46150	49798, 66811	a	0.562	1.125
46223	49798, 66811	a	0.694	1.038
47032	36512		1.042	0.884
47240	91316, 116003, 119608		0.440	0.933
47382	36512		0.652	0.954
73699	104337	c	0.401	0.947
73882	36861, 37043, 47839		1.020	1.041
74180	70761, 80404	d	0.826	-
75211	57060	a	0.772	1.124
75860	91316, 116003, 119608		1.423	0.850
80077	91316		2.416	0.836
93737	46300, 87737	d	0.436	-
93873	37128, 38771, 91316		0.958	0.904
111613	46300, 87737	d	0.616	-
112272	37128, 38771		1.445	1.005
112364	91316, 116003, 119608		0.552	0.770
148937	49798, 66811	a	0.888	0.997
152246	57682		0.535	0.888
152408	57060	a,b	0.523	0.853

Note to table 5: The following notes apply: (a) HeII4686 is in emission for Of stars. The effect on the magnitudes at 470.8 nm has been removed as far as possible, using literature data on line strengths, in combination with the known transmission characteristics of the filter. Calculated corrections apply relative to an absorption line of 0.6 Å equivalent width. (This choice was made only because two Of stars happened to have an absorption line of this width). For one star (HD 57060), the emission line strength was not known; in this case, the emission effect has been partly removed, by making a linear fit to the magnitudes at 449.6, 470.8 and 499.9 nm and reading off the value at 470.8 nm. Corrections for the individual stars (at 470.8 nm) were as follows: HD 57060: + 0.019, HD 66811: + 0.030, HD 148937: + 0.013, HD 152408: + 0.041, HD 46150: no corr. (line in absorption, equiv. width = 0.6 Å), HD 46223: no corr. (line in absorption, equiv. width = 0.6 Å), HD 75211: no corr. (no data on line strength; no clear effect visible on observed magnitude).
(Note: Table 3 contains the uncorrected values, for all stars). (b) HD 152408: probably there is also He line emission around 449.6 and 668.1 nm. No corrections were made for this, since no data on equivalent widths were available. (c) HD 73699: From analysis of Balmer discontinuity, it seems more appropriate to classify this star as B1.5 V. (d) HD 74180, 93737, 111613: UV extinction has not been calculated, because Balmer discontinuity is too strong to match accurately.

TABLE 6. *Interstellar extinction, normalized to* $m = 0.0$ *at* $1.5\ \mu^{-1}$, *and* $m = 1.0$ *at* $2.2\ \mu^{-1}$.

λ_0(nm)	$\lambda_0^{-1}(\mu^{-1})$	EXTINCTION									
		HD 46150	HD 46223	HD 47032	HD 47240	HD 47382	HD 73699	HD 73882	HD 74180	HD 75211	HD 75860
340.2	2.939	1.831	1.803	1.721	1.725	1.718	1.693	1.766	-	1.850	1.667
349.3	2.863	1.751	1.732	1.637	1.650	1.644	1.631	1.694	-	1.766	1.602
360.0	2.778	1.658	1.622	1.555	1.566	1.544	1.551	1.592	-	1.672	1.519
378.5	2.642	1.509	1.486	1.423	1.420	1.376	1.476	1.456	-	1.513	1.396
403.8	2.476	1.319	1.324	1.308	1.295	1.276	1.269	1.284	1.322	1.326	1.276
419.2	2.385	1.206	1.228	1.220	1.205	1.190	1.160	1.192	1.247	1.232	1.193
439.5	2.275	1.107	1.118	1.110	1.107	1.090	1.077	1.078	1.151	1.106	1.094
449.6	2.224	1.028	1.037	1.049	1.027	1.018	1.012	1.007	1.059	1.049	1.013
470.8	2.124	0.915	0.912	0.919	0.907	0.905	0.898	0.898	0.885	0.918	0.900
499.9	2.000	0.731	0.723	0.731	0.718	0.741	0.756	0.739	0.702	0.742	0.742
520.5	1.921	0.594	0.591	0.590	0.598	0.604	0.613	0.621	0.598	0.602	0.618
540.7	1.849	0.493	0.480	0.473	0.505	0.491	0.509	0.509	0.458	0.481	0.507
560.1	1.785	0.379	0.375	0.367	0.391	0.379	0.392	0.410	0.364	0.367	0.392
582.1	1.718	0.306	0.300	0.298	0.309	0.307	0.317	0.320	0.286	0.271	0.301
610.7	1.637	0.165	0.186	0.194	0.182	0.199	0.197	0.210	0.196	0.167	0.190
640.0	1.563	0.109	0.092	0.079	0.102	0.107	0.125	0.104	0.092	0.078	0.099
668.1	1.497	-0.005	-0.001	0.007	0.005	0.011	-0.012	-0.007	0.006	-0.003	0.004
710.2	1.408	-0.085	-0.107	-0.145	-0.150	-0.123	-0.107	-0.136	-0.126	-0.102	-0.139
750.5	1.332	-0.208	-0.242	-0.248	-0.216	-0.210	-0.299	-0.254	-0.217	-0.245	-0.237
787.3	1.270	-0.375	-0.318	-0.274	-0.341	-0.385	-	-0.353	-0.310	-0.288	-0.341

λ_0(nm)	$\lambda_0^{-1}(\mu^{-1})$	EXTINCTION									
		HD 80077	HD 93737	HD 93873	HD 111613	HD 112272	HD 112364	HD 148937	HD 152246	HD 152408	weighted average
340.2	2.939	1.676	-	1.699	-	1.762	1.601	1.761	1.699	1.704	1.725
349.3	2.863	1.604	-	1.627	-	1.681	1.534	1.686	1.622	1.639	1.651
360.0	2.778	1.517	-	1.527	-	1.566	1.466	1.601	1.536	1.568	1.559
378.5	2.642	1.409	-	1.409	-	1.430	1.391	1.461	1.407	1.428	1.431
403.8	2.476	1.286	1.287	1.268	1.295	1.287	1.239	1.305	1.288	1.315	1.292
419.2	2.385	1.204	1.213	1.199	1.219	1.202	1.167	1.206	1.198	1.231	1.206
439.5	2.275	1.089	1.096	1.092	1.115	1.099	1.094	1.098	1.097	1.094	1.100
449.6	2.224	1.019	1.023	1.026	1.041	1.043	1.020	1.033	1.026	0.979	1.027
470.8	2.124	0.903	0.906	0.916	0.911	0.931	0.900	0.909	0.921	0.864	0.907
499.9	2.000	0.736	0.741	0.739	0.753	0.745	0.723	0.741	0.753	0.792	0.738
520.5	1.921	0.611	0.606	0.597	0.607	0.594	0.596	0.601	0.615	0.673	0.606
540.7	1.849	0.498	0.495	0.492	0.474	0.475	0.507	0.486	0.482	0.526	0.491
560.1	1.785	0.398	0.394	0.396	0.359	0.358	0.397	0.378	0.368	0.402	0.383
582.1	1.718	0.308	0.310	0.311	0.278	0.280	0.328	0.310	0.293	0.289	0.301
610.7	1.637	0.196	0.170	0.203	0.162	0.189	0.194	0.180	0.194	0.214	0.190
640.0	1.563	0.108	0.094	0.098	0.099	0.093	0.107	0.106	0.071	0.088	0.098
668.1	1.497	0.000	-0.014	-0.003	-0.008	0.004	0.016	-0.012	-0.022	-0.090	-0.004
710.2	1.408	-0.125	-0.135	-0.177	-0.114	-0.129	-0.112	-	-	-	-0.128
750.5	1.332	-0.239	-0.264	-0.267	-0.226	-0.224	-0.243	-0.224	-0.191	-0.216	-0.236
787.3	1.270	-0.354	-0.289	-0.276	-0.302	-0.311	-0.373	-	-	-	-0.327

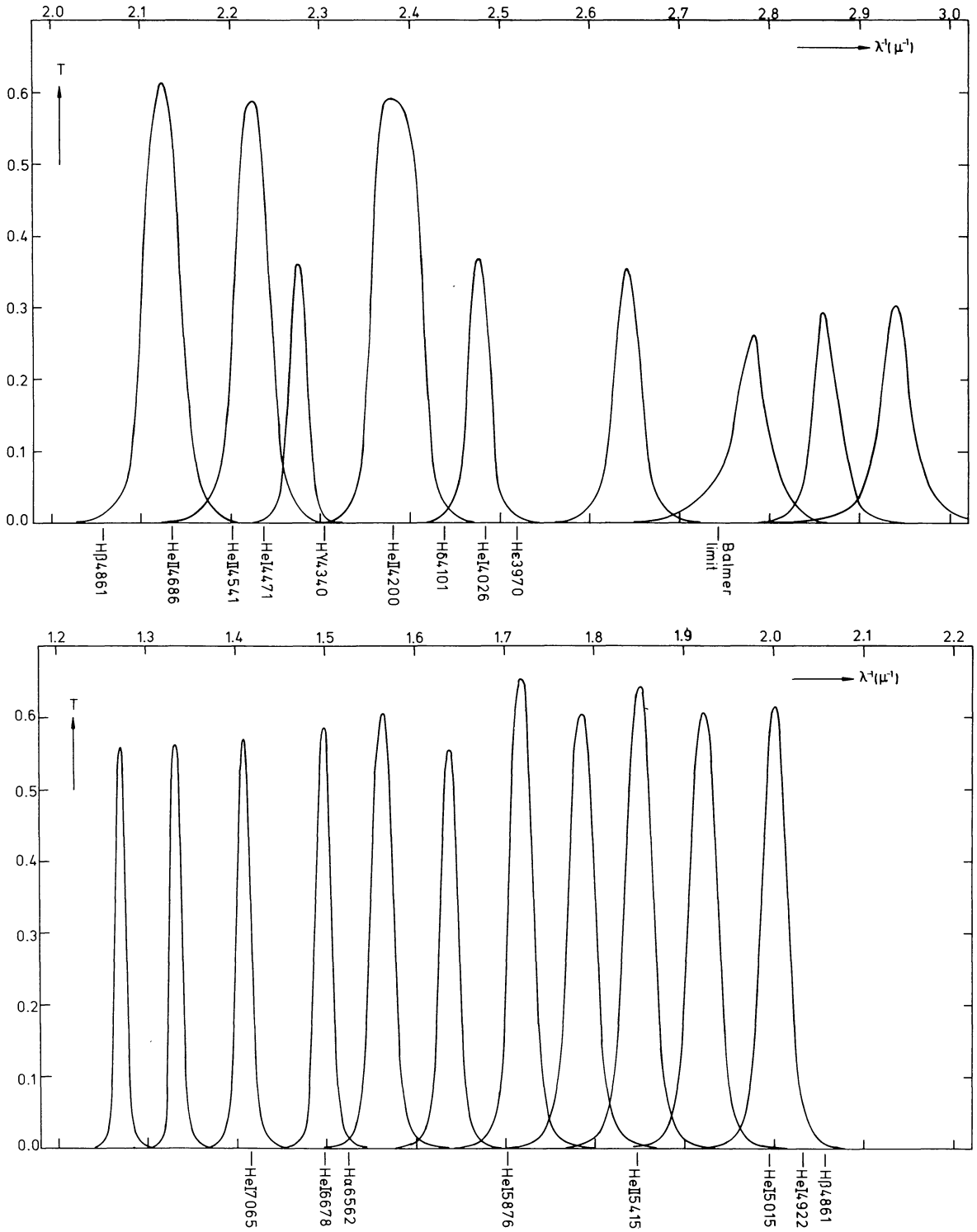

FIGURE 1. Filter transmission factor T as a function of λ^{-1}. The main line features within and near the passbands are indicated.

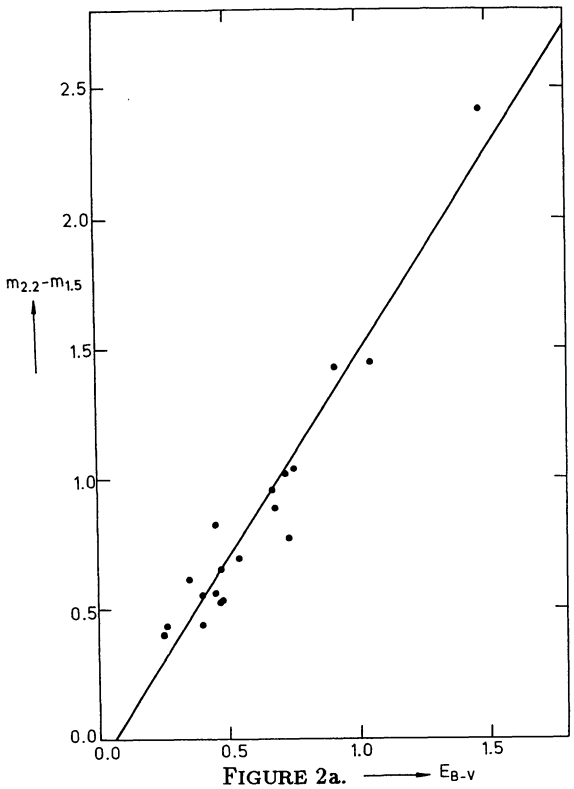

FIGURE 2a.

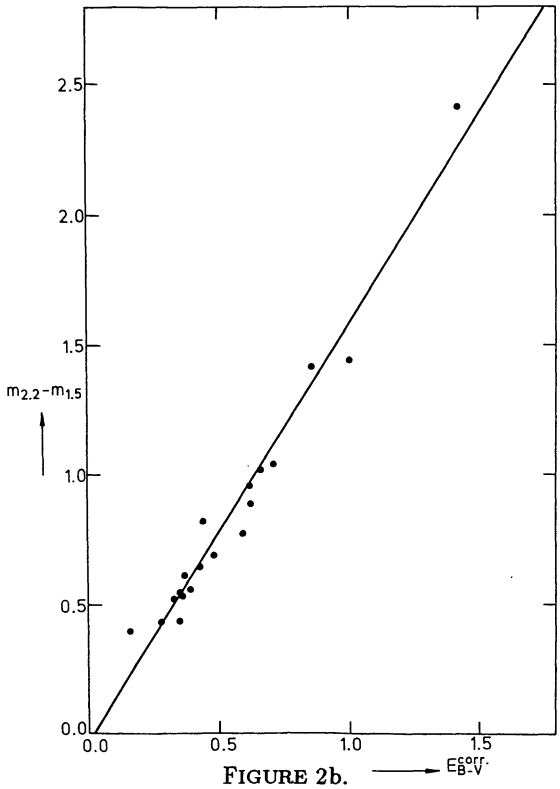

FIGURE 2b.

FIGURE 2. Color excess $m_{2.2} - m_{1.5}$ plotted against E_{B-V} (Fig. 2a) and against E^{corr}_{B-V} (Fig. 2b). $E^{corr}_{B-V} = E_{B-V} - E^{0}_{B-V}$, where E^{0}_{B-V} is the residual color excess of the average unreddened comparison star used. Correlation with E^{corr}_{B-V} is marginally better.

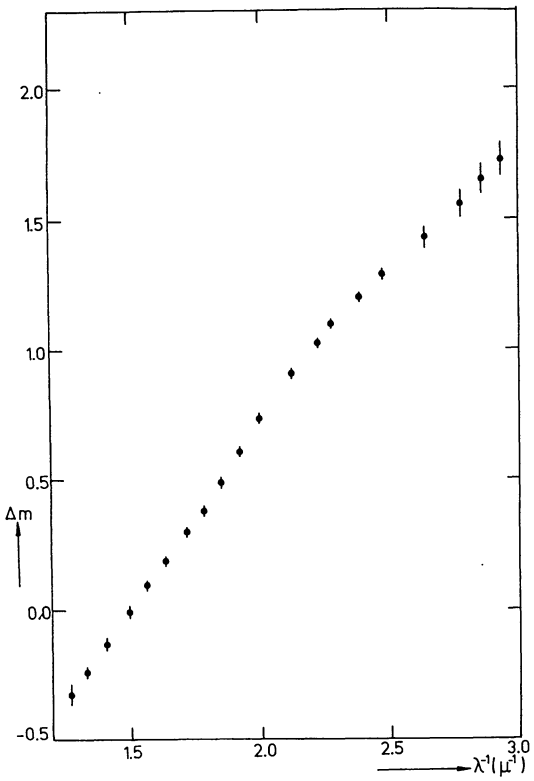

FIGURE 3. Weighted mean normalized interstellar extinction curve, based on 19 stars. Error bars indicate standard deviation (not mean error!) to illustrate the spread in individual extinction curves.

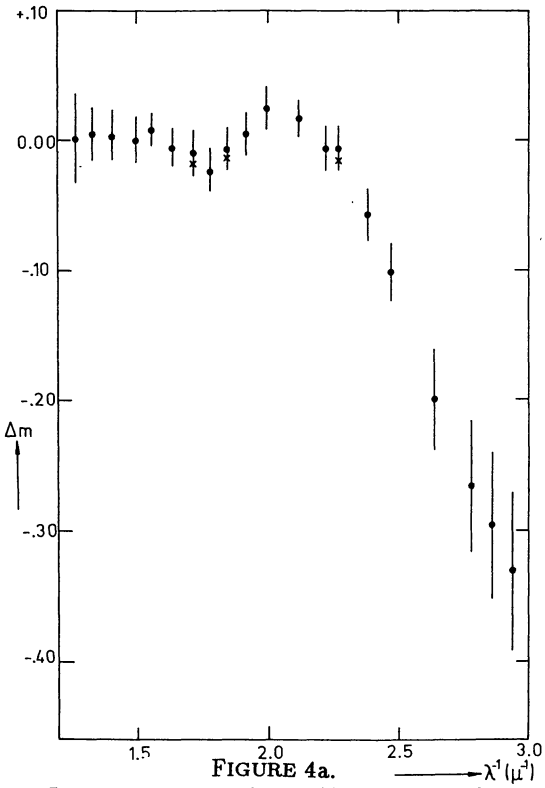

FIGURE 4a.

FIGURE 4. Interstellar extinction residuals, after subtraction of a straight line through the extinction normalization points at $\lambda^{-1} = 1.5$ and 2.2 μ^{-1}. (a). Average residuals over 19 stars. Error bars represent standard deviation of individual stars around mean. Crosses (x) denote points corrected for diffuse interstellar bands. (b). Residuals for 2 individual stars. Error bars represent mean error and are indicated only when larger than 0.006; see text.

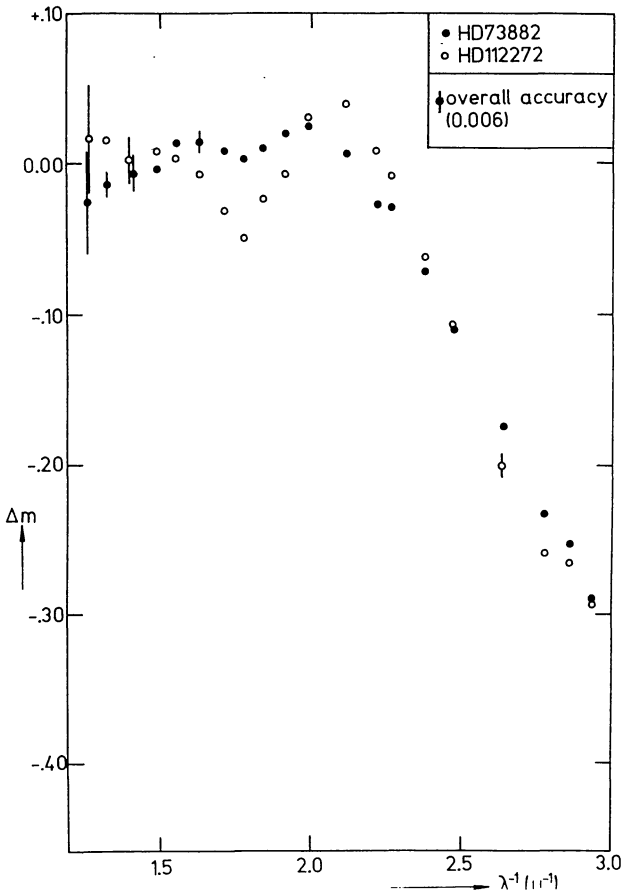

FIGURE 4b.

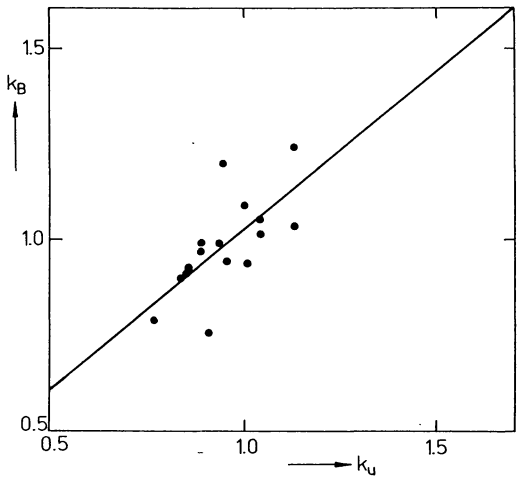

FIGURE 5. Influence of Balmerjump mismatch on the slope of the UV extinction curve. Slope k_u is based upon 6 wavelength points ($2.385-2.939\ \mu^{-1}$). Slope k_b is based upon 2 wavelength points ($2.385-2.476\ \mu^{-1}$).

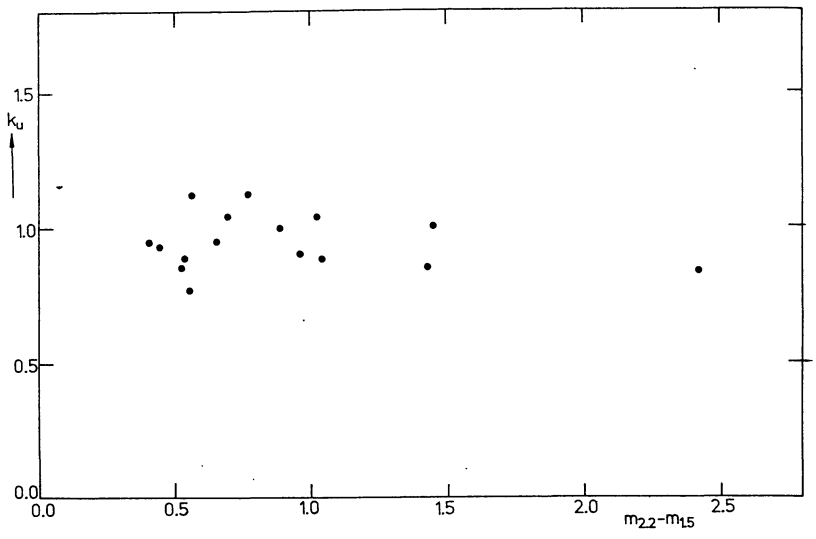

FIGURE 6. Slope k_u of the UV extinction curve, *versus* color excess.

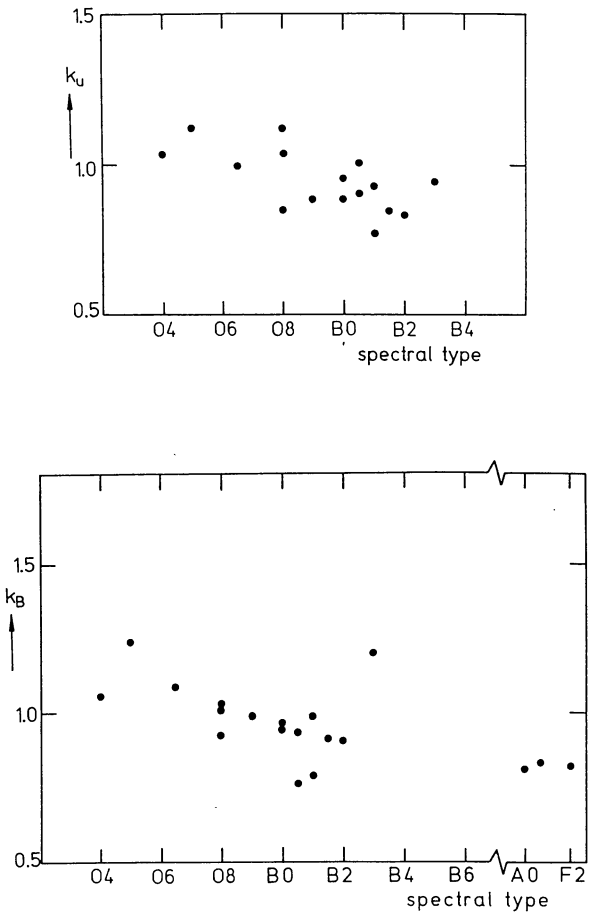

FIGURE 7. (a). Slope k_u of the UV extinction curve ($2.385 - 2.939\ \mu^{-1}$) *versus* spectral type of the star being observed. (b). Slope k_b of the UV extinction curve ($2.385 - 2.476\ \mu^{-1}$) *versus* spectral type of the star being observed.